Random-sequential adsorption of disks of different sizes

Paul Meakin
Department of Physics, University of Oslo, Box 1048, Oslo 0316, Norway

Remi Jullien
Laboratoire de Physique des Solides, Université Paris–Sud, Centre d'Orsay, 91405 Orsay, France
(Received 13 January 1992)

The random-sequential adsorption of disks with two or more sizes onto a planar substrate has been investigated using computer simulations. For a binary mixture of large and small disks, we find that the large-disk coverage reaches its asymptotic value exponentially, while the small disk reaches its asymptotic value algebraically according to Feder's law. For a uniform distribution of disk radii, the total coverage approaches its asymptotic value algebraically [$\rho(\infty)-\rho(t)\sim t^{-p}$, where $\rho(t)$ is the coverage at time t], but the characteristic exponent p has an effective value smaller than $\frac{1}{2}$. If the distribution of disk radii from which the disks are selected for attempted addition is Gaussian, then the exponent p has a very small effective value, and the distribution of adsorbed disks becomes very non-Gaussian if the initial Gaussian distribution is broad. Many of our simulation results can be understood in terms of the theoretical work of Talbot, Tarjus, and Schaff [Phys. Rev. A **40**, 4808 (1980)], but other aspects of this work are beyond current theoretical approaches.

PACS number(s): 68.10.Jy, 05.40.+j, 05.70.Ln, 02.50.+s

INTRODUCTION

Random-sequential adsorption (RSA) is one of the most simple and fundamental problems in statistical physics. In this process objects are added randomly, one at a time, to a d-dimensional space or lattice with the restriction that they must not overlap with previously added objects. As the process proceeds it becomes more and more difficult to find regions to which the objects can be added, and eventually (in the "jamming" limit) no further additions are possible. For sufficiently large systems this jamming limit can be characterized by the fraction of space [$\rho(\infty)$] covered by the deposited objects. The one-dimensional ($d=1$) model in which segments of equal length are added to a line is known as the "car parking" problem. A discretized (lattice) version of this model has been used to represent intramolecular reactions of linear polymers [1,2] and the oxidation of polysaccharides [3]. Similar models in which the adsorbed object may occupy more than one lattice site has been used to represent the binding of large ligands (polypeptides, dye molecules, antibiotics, etc.) to linear macromolecules [4]. It has also been suggested that the continuum model can be applied to the adsorption of linear molecules into parallel troughs [5].

In the two-dimensional case lattice models have been used to describe the adsorption and reaction of small molecules on flat surfaces [6–8]. The most successful application is that of the off-lattice random-sequential disk adsorption model [10–12] to the adsorption of globular macromolecules [13] and polymer microspheres [14,15].

In the three-dimensional case, work on random-sequential sphere-packing simulations [16–19] has been motivated in part by the idea that this model might contribute to our understanding of the physics of fluids and other amorphous materials. However, this is not a very realistic model for this purpose [20].

A variety of exact theoretical results have been obtained for one-dimensional random-sequential-adsorption problems [1–3,20–22]. In two dimensions exact results have been obtained for a number of lattice models [6,23,24], but there has been relatively little progress on even the most simple off-lattice models. Motivated by the results of one- and two-dimensional computer simulations, Feder [12] proposed that the asymptotic approach of the surface coverage $\rho(t)$ to its asymptotic ($t\rightarrow\infty$) value $\rho(\infty)$ could be described by

$$\rho_d(\infty)-\rho_d(t)\sim t^{-1/d}\ , \tag{1}$$

where t is the time and d is the dimensionality. Here t is to be interpreted in terms of a scenario in which objects are added randomly, at a constant rate, to a d-dimensional substrate and accepted by the substrate only if they do not overlap previously adsorbed objects. The time t may then be measured in terms of the number of attempted additions per unit length (area, volume, etc.) or the coverage that would be attained if overlap was allowed and all attempted additions were accepted. Theoretical arguments supporting Feder's law [Eq. (1)] have been presented by Swendsen [25] and Pomeau [26]. Feder's law appears to be valid for the random-sequential adsorption of hyperspheres [17,18,27] but not for randomly oriented elipses [28] and rectangles [29] or parallel squares [25,30].

Recently, there has been a resurgence of interest in random-sequential-adsorption models [29–49]. Much of this recent work is concerned with the adsorption of an-

isometric particles on continuous two-dimensional substrates. For these systems it appears that the approach to the asymptotic coverage can be described in terms of generalization of Eq. (1):

$$\rho(\infty)-\rho(t)\sim[\ln(t)]^{q}t^{-p}\ . \tag{2}$$

Some of the more recent work was also concerned with the adsorption of rectangles with a width of one lattice unit and two different lengths l_1 and l_2 lattice units where l_1 and l_2 are integers) onto a square lattice. Very recently [49] Bartelt and Privman have obtained an exact solution for the case $l_1=1$, $l_2\rightarrow\infty$.

In general there has been very little attention given to the problem of the random-sequential adsorption of disks or spheres of different sizes despite the fact that this is a problem that is amendable with experimental study and some of the most important random-sequential examples involve the adsorption of macroscopic particles that are not perfectly monodisperse. Talbot and co-workers [46,47] have carried out theoretical studies of the RSA process for binary mixtures and polydisperse mixtures. The work on binary mixtures is concerned with the RSA of disks of very different sizes [46] and the work on polydisperse mixtures [47] is concerned with the asymptotic approach to the jamming limit.

Here we report the results obtained from computer simulations carried out using a two-dimensional substrate with disks of two or more radii. Most of our work has been devoted to three models: (i) the deposition of disks with two different radii (r_A and r_B with $r_A<r_B$), (ii) the deposition of disks with radii uniformly distributed over the range $r_A<r<r_B$, and (iii) the deposition of disks with radii selected from a truncated Gaussian distribution.

COMPUTER SIMULATIONS

All of the simulations were carried out using an underlying lattice with a size of $L\times L$ lattice units. In general the disk radii are distributed over the range $r_A<r<r_B$ and the radius of the smallest disk was selected to be 0.7075 (slightly larger than $1/\sqrt{2}$ so that the center of at most one disk can lie within any particular cell of the underlying lattice). The random-sequential-adsorption algorithm used in this work consists of selecting one of the lattice cells at random and the selecting a point within the selected lattice cell at random. A disk radius is then selected at random from the distribution of radii and an attempt is made to add a disk with this radius so that its center lies at the randomly selected point. Each element in the underlying lattice that is occupied by the center of a disk is labelled with a number that points to the position of that disk in a list of disk radii and coordinates. This facilitates the process of checking for overlap between the selected disk and disks that have previously been deposited. (The search can be restricted to neighboring disks by searching for contacts with only those disks whose centers lie in lattice cells with x or y coordinate lying within a distance of $r_{\max}+r_s+1$ lattice units from the x or y coordinates, respectively, of the selected cell. Here $r_{\max}$ is the maximum radius for any previously deposited disk and r_s is the radius of the selected disk.) If no overlaps are found, the selected disk is added to the list of disk coordinates, and the radii and the selected cell on the underlying lattice are updated so that the disk can easily be located in subsequent overlap checks. If an overlap is detected in a new lattice cell, trial position and radius are selected and the procedure described above is repeated.

The algorithm described above can be improved slightly (by a factor of 2–3) by selecting only "active" lattice cells in which deposition is still possible. This requires a check of those cells in the vicinity of each newly deposited disk to determine which sites, if any, are occluded by the newly deposited disk. A list of active lattice cells must also be maintained and updated. This adds little complexity to the algorithm and the additional storage requirements for the list of active sites does not present a serious problem.

In these simulations we did not attempt to reach the jamming limit. Instead, we relied on Feder's law or a suitable generalization [Eq. (2)] to estimate the asymptotic coverage density $\rho(\infty)$ and radius distribution $N_r(\infty)$. Here $N_r(t)\delta r$ is the number of disks with radii in the range r to $r+\delta r$ at time t. To do this (and to explore the kinetics of the random-sequential-adsorption process) a time scale must be maintained. In these models the time t is gradually increased by an amount δt given by

$$\delta t=\pi r_s^{\,2}/L^2 \tag{3}$$

each time an attempt is made to deposit a disk of radius r_s. If N_A sites are still active and addition is attempted only in still active cells, then the time increment is given by

$$\delta t=\pi r_s^{\,2}/N_A\ . \tag{4}$$

An alternative way of introducing a time scale into these simulations would be to gradually increase the time (t') by a constant amount ($\delta t'$) each time an attempt was made to add a new particle to the substrate. In this version of the model, Eq. (3) would be replaced by $\delta t'=1/L^2$ and Eq. (4) by $\delta t'=1/N_A$. The times t and t' are linearly related to each other ($t=\pi\langle r_s^2\rangle t'$) and both correspond to the physical time scale for an experiment in which a constant flux of particles impinges randomly on a sticky substrate.

As a check on the algorithms used in this work more than fifty simulations were carried out in which 10^8 or 2×10^8 attempts were made to deposit monodisperse disks in an area of size 512×512. In the later stages of the process the surface coverage could be described very well by Eqs. (1) and a value of 0.5467 ± 0.0003 was found for $\rho_2(\infty)$ by fitting $\rho_2(t)$ by Eq. (1). This result is in good agreement with the value of 0.5473 ± 0.0009 reported by Tanemura [10] and the value of 0.5472 ± 0.0002 obtained by Hinrichsen and co-workers [27,48].

RESULTS

Binary mixtures

Simulations were carried out for mixtures of particles of two different sizes ($r_A = 0.7075$ and $r_B = Rr_A$) with values for the radius ratio parameter (R) lying in the range $1.125 < R < 8$. For each value of R, simulations were carried out using a range of values for the parameter f, which is the fraction of small disks selected for trial deposition onto the substrates. In most cases ten values of f in the range of 0.016 to 0.875 were used. For the smaller values of f most simulations were carried out on systems of size $L = 512$ and in most cases $L = 1024$ for the larger values of R.

Figure 1 shows deposition patterns obtained with equal numbers of large and small disks ($f = \frac{1}{2}$) and four different values for the radius ratio ($R = 1.5$, 2.0, 4.0, and 8.0). It is, of course, not surprising to find that the fraction of small disks that are successfully absorbed increases as the ratio R increases.

Figure 2 shows the time dependence of the small-disk coverage [$\rho_S(t)$] and the large-disk coverage [$\rho_L(t)$] obtained from simulations carried out with the parameter $R = 4$ and $f = \frac{1}{2}$. Figure 2(a) shows that ρ_L rapidly ap-

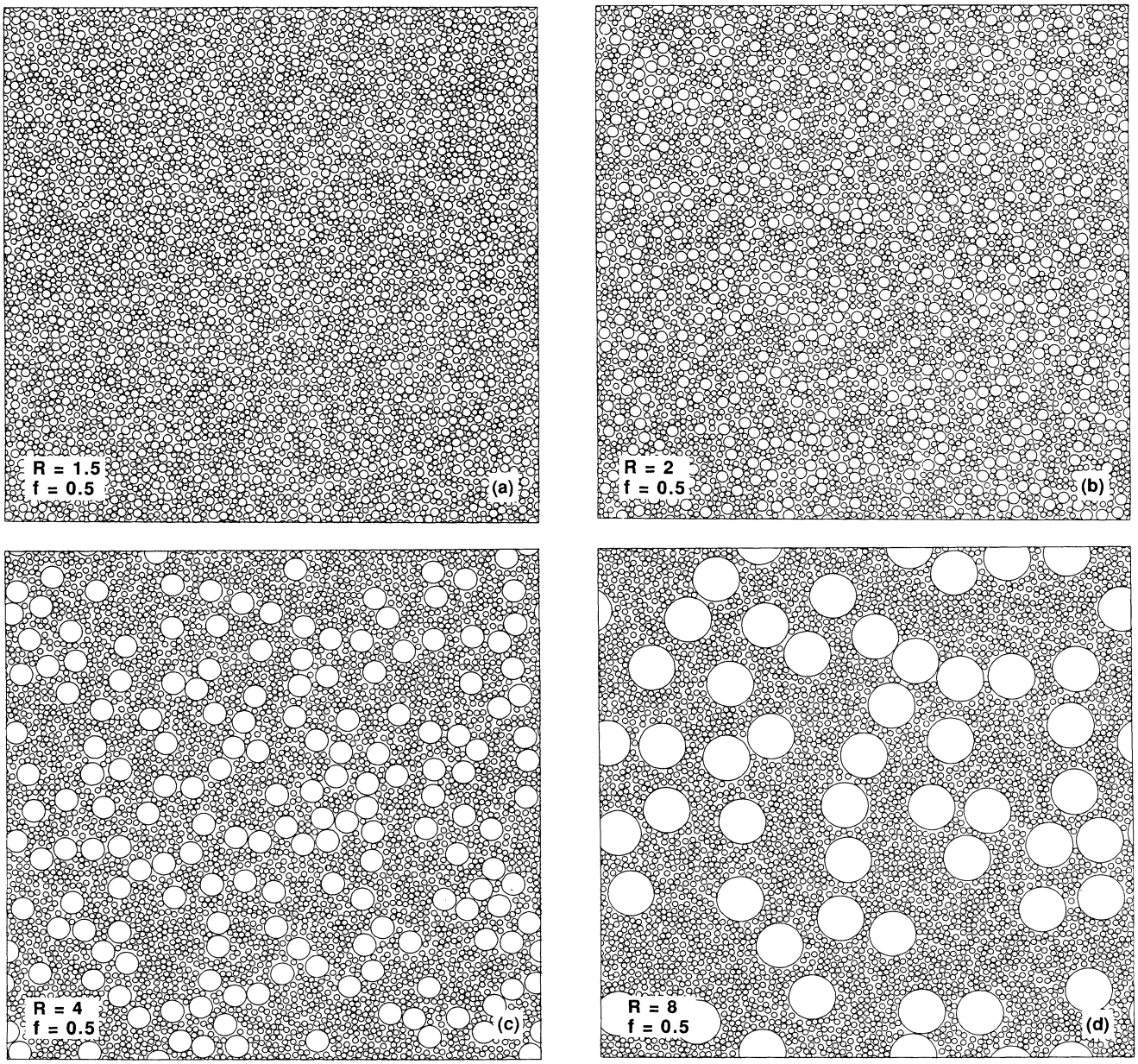

FIG. 1. Patterns generated by the binary mixture model with an equal number of large and small disks selected for trial deposition. (a), (b), (c) , and (d) show configurations generated with radius ratio r of 1.5, 2.0, 4.0, and 8.0 near to the jamming limit. In these small-scale simulations the radius of the small disks was 0.7075 and the system size was 128×128.

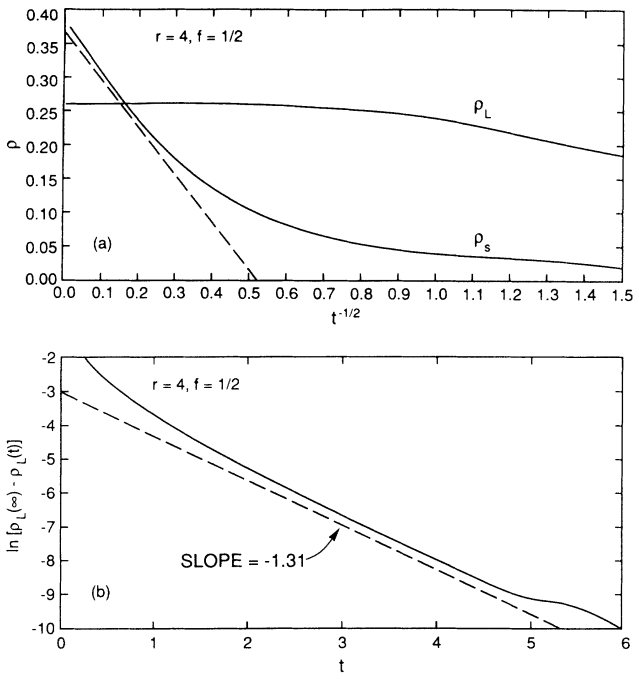

FIG. 2. Time dependence of the coverages ρ_S and ρ_L for small and large disks obtained from a simulation carried out using the binary RSA model. Here time is measured in units of the coverage $(\rho_S+\rho_L)$ that would be obtained if all the disks were accepted.

proaches a constant value but ρ_S approaches its limiting value much more slowly. Figure 2(a) indicates that $\rho_S(t)$ obeys Feder's law [Eq. (1)], while Fig. 2(b) shows that $\rho_L(t)$ approaches its asymptotic value exponentially:

$$\rho_L(t)=\rho_L(\infty)-ae^{-kt} . \tag{5}$$

This behavior appears to be characteristic for all values of R and f but it is more difficult to demonstrate for $R \rightarrow 1$. Talbot and Schaaf [46] have shown that $\rho_L(t)$ approaches its asymptotic value exponentially [Eq. (5)], while $\rho_S(t)$ approaches it asymptotic value algebraically [Eq. (1)] for $R \gg 1$. Because $\rho_L(t)$ approaches its asymptotic value much more rapidly than $\rho_S(t)$, only small particles can be added in the final stages of the binary RSA process. The simulations can be made more efficient by attempting to add only small disks after the probability that a large disk will be accepted has decayed to an essentially zero value. Advantage was taken of this in some of our simulations (particularly those with large values for R and small f values for which the benefit is the largest).

The dependence of the asymptotic values of the disk coverages $[\rho_S(\infty)$ and $\rho_L(\infty)]$ and the "decay constant" (k) in Eq. (5) on the model parameters R and f are of obvious interest. $\rho_L(\infty)$ can easily be determined by simply measuring $\rho_L(t)$ in the saturated regime $(t \gg k^{-1})$. The asymptotic small-disk coverage was obtained by extrapolating $\rho_S(t)$ to $t=\infty$ assuming that Feder's law is obeyed. This procedure is supported by our simulation results [Fig. 2(a), for example].

Figure 3 shows the dependence of $\rho_S(\infty)$, $\rho_L(\infty)$, and $\rho_T(\infty)$ (ρ_T is the total coverage $\rho_S+\rho_L$) on the composition parameter f for four values of R (1.5, 2.0, 4.0, and 8.0). For each value of R simulations were carried out for ten values of f (0.016, 0.03125, 0.0625, 0.125, 0.25, 0.375, 0.5, 0.625, 0.75, and 0.875). The highest total cov-

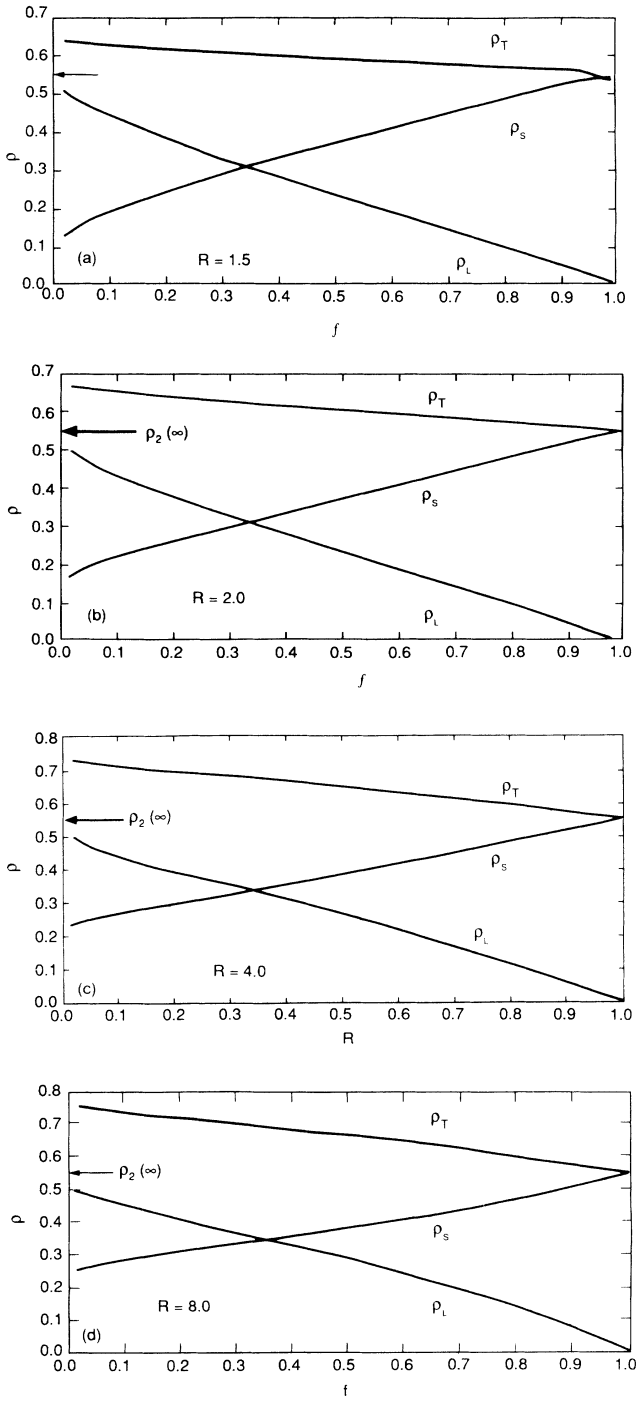

FIG. 3. Dependence of the surface coverages ρ_S, ρ_L, and ρ_T on the fraction of small disks (f) that are "fed" to the surface. (a), (b), (c), and (d) show results for $R=1.5$, 2.0, 4.0, and 8.0, respectively.

erage is obtained for $f \to 0$. In this limit the large disks are added until the jamming limit is reached [$\rho_L \to \rho_2(\infty)$], then the gaps between the large disks are filled with smaller disks. In the limit $r \to \infty$ the total coverage as $f \to 0$ is given by

$$\rho_T = \rho_2(\infty) + [1 - \rho_2(\infty)]\rho_2(\infty) , \tag{6}$$

which gives a value of 0.7945 if $\rho_2(\infty)$ is 0.5467. In this same limit ($R \to \infty$, $f \to 0$) the small-disk coverage is expected to approach a value given by

$$\rho_S = [1 - \rho_2(\infty)]\rho_2(\infty) , \tag{7}$$

or 0.2478 for $\rho_2(\infty) = 0.5467$. As R becomes smaller (in the $f \to 0$ limit) there is less space for the small disks after the large disks have been adsorbed and we expect that $\rho_S \to 0$ as $R \to 1.0$. Unfortunately, it becomes difficult to obtain reliable values for ρ_S as this limit is approached [see Fig. 3(a)].

Talbot and Schaaf [46] have obtained an approximate theoretical result for $\rho_L(\infty)$ that becomes exact in the limit $R \to \infty$ and is accurate for large R and sufficiently large values of f ($f \gtrsim 0.45$). A comparison of the theoretical predictions of Talbot and Schaaf with our simulation results for $R = 8$ and for values of f in the range $0.5 < f < \frac{5}{6}$ [see Fig. 3(d) and Fig. 2 in Ref. [46]] indicate a satisfactory agreement between the simulations and theoretical results.

The simulations described above were augmented by additional simulations that were carried out to explore the dependence of $\rho_S(\infty)$ and $\rho_L(\infty)$ on the radius ratio (R). Results for $R = 0.125$, 0.5, and 0.875 are shown in Fig. 4. It is apparent from Fig. 4 that $d[\rho_L(\infty)]/dR$ and $d[\rho_S(\infty)]/dR$ diverge as $R \to 1$. However, very accurate values for $\rho_L(\infty)$ and $\rho_S(\infty)$ are needed to study the behavior as $R \to 1$. A quite extensive series of simulations was carried out in an attempt to determine how $\rho_S(\infty)$ and $\rho_L(\infty)$ approach the $R \to 1$ limit. Figures 4(d) and 4(e) show the dependence of $\ln[|\rho_S(\infty, R) - \rho_S(\infty, 1)|]$ on $\ln(R-1)$ and $\ln[|\rho_L(\infty, R) - \rho_L(\infty, 1)|]$ on $\ln(R-1)$ for the $f = 0.125$, 0.50, and 0.875 simulations. These results suggest that

$$|\rho(\infty, R) - \rho(\infty, 1)| \sim (R-1)^{\alpha} . \tag{8}$$

The effective value of the exponent α appears to increase with increasing f and effective values of 0.55, 0.75, and 0.95 were obtained for $f = 0.125$, 0.50, and 0.875, respectively. These results suggest that the exponent α might increase linearly from a value of 0.5 for $f \to 0$ to a value of 1.0 for $f \to 1.0$. However, because of the difficulty of approaching the $t \to \infty$ limit for $R \to 1$ and the accuracy needed for $R \to 1$ [where $\rho(R, \infty) \simeq \rho(1, \infty)$], we cannot completely eliminate the possibility that α has a universal (f-independent) asymptotic value. For the smallest values of R a total of about 10^{10} attempted additions was used for each data point in Fig. 4. Larger-scale simulations would be needed to determine unambiguously if the exponent α depends on the composition parameter f. Such simulations would be beyond our present resources.

In the simulations described above, almost all the com-

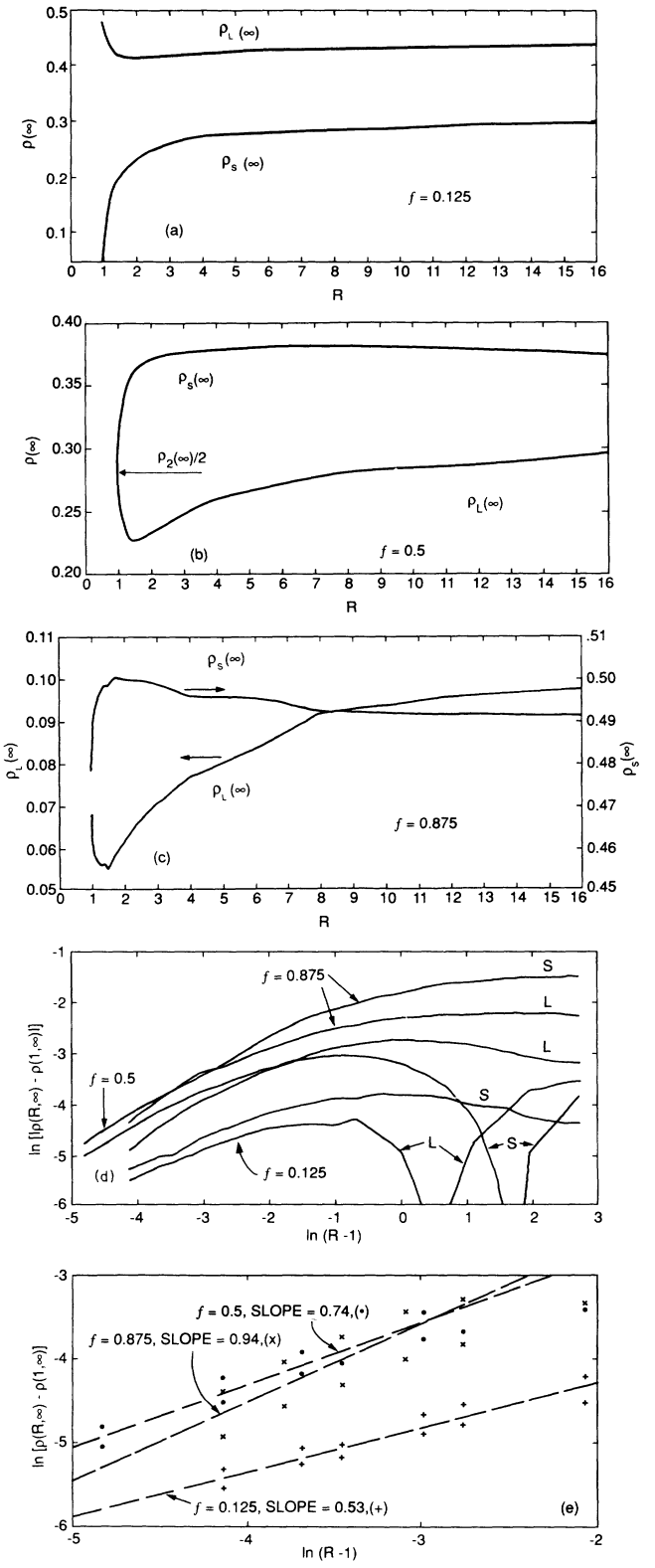

FIG. 4. Dependence of the asymptotic coverages [$\rho_S(\infty)$ and $\rho_L(\infty)$] on the radius ratio (R) obtained from the binary RSA model. (a), (b), and (c), show results from simulations in which the fractions of small disks (f) that are fed to the surface are 0.125, 0.50, and 0.875, respectively. (d) and (e) show the dependence of $\ln[\rho_S(R, \infty) - \rho_S(1, \infty)]$ and $\ln[\rho_L(R, \infty) - \rho_L(1, \infty)]$ on $\ln(R-1)$ for $f = 0.125$, 0.5, and 0.875.

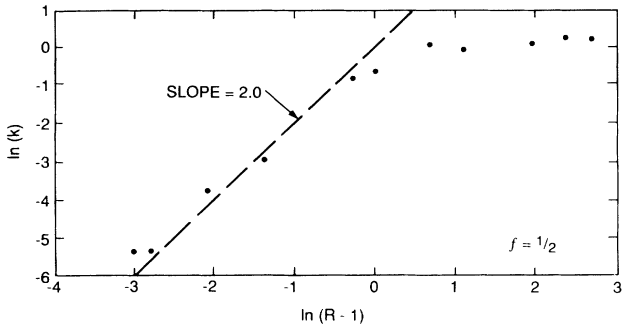

FIG. 5. Dependence of the constant k in Eq. (5) describing the exponential approach of $\rho_L(t)$ to its asymptotic value on the radius ratio parameter (R) for the random-sequential adsorption of binary mixtures.

puter time was spent adding small disks after the large-disk coverage had reached its asymptotic value. Consequently, additional simulations were carried out with much fewer attempted depositions (except for small values of R) to obtain more accurate values for the constant k in Eq. (5) that describe the exponential approach of $\rho_L(t)$ to its asymptotic value. Figure 5 shows the dependence of k on the disk radius ratio (R) for simulations carried out with $f=0.5$. The result shown in Fig. 5 suggest that

$$k \sim (R-1.0)^2 \tag{9}$$

for small value of R and that k has a constant value of order 1 for large values of R. For very small values of R the constant k has a small value that is difficult to measure accurately.

Uniform radius distribution

A series of simulations was carried out in which the radii of the disks were selected randomly from a uniform distribution over the range $r_A < r < r_B$. For this model the width of the distribution can be defined in terms of the parameter $R' = r_B / r_A$. Figure 6 shows the size distribution $[N_r(t)]$ at several stages during simulations carried out with size distribution parameters (R') of 1.25, 2.0, and 8.0. Here $N_r(t)\delta r$ is the number of disks with radii in the range of r to $r+\delta r$ at time t. The distribution has a maximum at $r = r_A$ and the asymptotic distribution (in the limit $t \to \infty$) becomes more strongly peaked at $r = r_A$ as the size distribution becomes broader.

As in the other simulations we have measured the time dependence of the total coverage (ρ_T). We find that for large values of the time (t) the dependence of ρ_T on t cannot be described by Eq. (1) with $d=2$. This can be demonstrated in several ways. In Fig. 7 the dependence of $\ln[\rho_a(\infty)-\rho(t)]$ on $\ln(t)$ is shown for $R'=1.25$, 2.0, and 8.0. Here $\rho_a(\infty)$ is a test value for the asymptotic coverage. The results in Fig. 7 suggest that for large t the total coverage $\rho(t)$ can be described in terms of an equation with the same form as Eq. (1) but with a different exponent

$$\rho(\infty)-\rho(t) = t^{-p} . \tag{10}$$

Figure 7 shows the dependence of $\ln[\rho_a(\infty)-\rho(t)]$ on $\ln(t)$ for several values of $\rho_a(\infty)$ for each value of R'. A straight line with a slope of $-p$ would correspond to Eq. (10). The results shown in Fig. 7 and results from other simulations suggest that the effective value of the exponent p varies continuously with R'. In the limit $R' \to 1$ we know that $p = \frac{1}{2}$. However, it is not clear if the effective values we find for p represent the true asymptotic behavior or if they are a consequence of a crossover to a constant exponent for all $R' > 1$ at large enough times. The theoretical work of Tarjus and Talbot [47] indicates that Eq. (1) should be replaced by

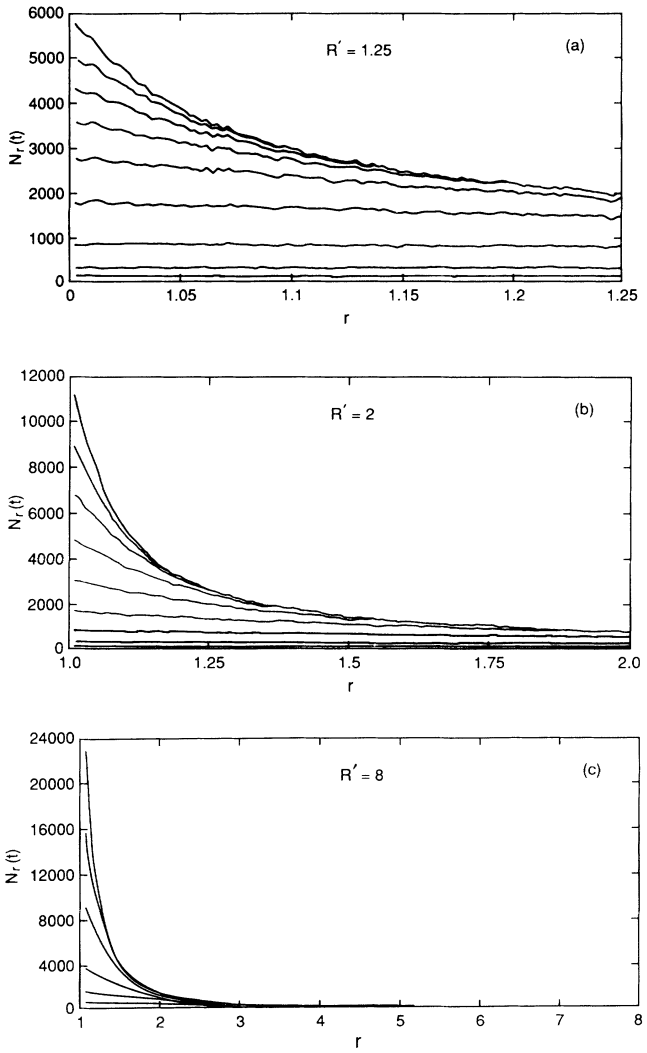

FIG. 6. Dependence of the adsorbed radius distribution at various stages during polydisperse RSA simulations. The simulations were carried out by attempting to add disks with radii uniformly distributed over the range $r_A < r < r_B$. (a), (b), and (c) show distributions for $R'=1.25$, 2.0, and 8.0, respectively, where $R' = r_B / r_A$. The time was increased by a factor of about 3.6 between each distribution and results from several simulations were averaged.

$$\rho_T(\infty)-\rho_T(t)\sim t^{-1/(d+1)} \tag{11}$$

for the disk size distribution used in this work. The value of 3 predicted for the exponent p in Eq. (10) is consistent with our simulation results for small values of R' but a larger effective value is found for large values of R'. This observation may also be understood in terms of the theoretical results of Tarjus and Talbot [47]. If the distribution function for the radii of the disks that we attempt to add to this surface has a value of zero but the nth derivative of the distribution is nonzero at $r=r_A$, then the exponent p in Eq. (10) is given by [47]

$$p=1/(d+1+n)\ . \tag{12}$$

Consequently, for a very broad uniform distribution we might expect an effective value of $\frac{1}{4}$ for p crossing over to a value of $\frac{1}{3}$ very close to the jamming limit. This idea seems to be consistent with our simulation results.

In Fig. 8 the dependence of $\ln(N_r)$ on $\ln\{[100(r-r_A)]/[(R'-1)r_A]\}$ is shown at several different stages during simulations carried out with radius ratio (R') of 1.25, 2.0, and 8.0. Figures 6 and 8 show that the disk number distribution (N_r) reaches a stationary (time-dependent) form for the larger disk sizes in these simulation. The results in Fig. 8 indicate that N_r has the form

$$N_r\sim(r-r_A)^{-\gamma}\ , \tag{13}$$

where the exponent γ depends on the size distribution R'. Since a value greater than 1 for the exponent γ would imply an infinite surface coverage and the effective value of γ is much larger than 1 [Fig. 8(c)] for some value of R' it is apparent that Eq. (13) cannot correctly describe the adsorbed disk size distribution over the entire range of disk sizes ($r_A<r<r_B$). Simulations were carried out for other values of the polydispersity parameter

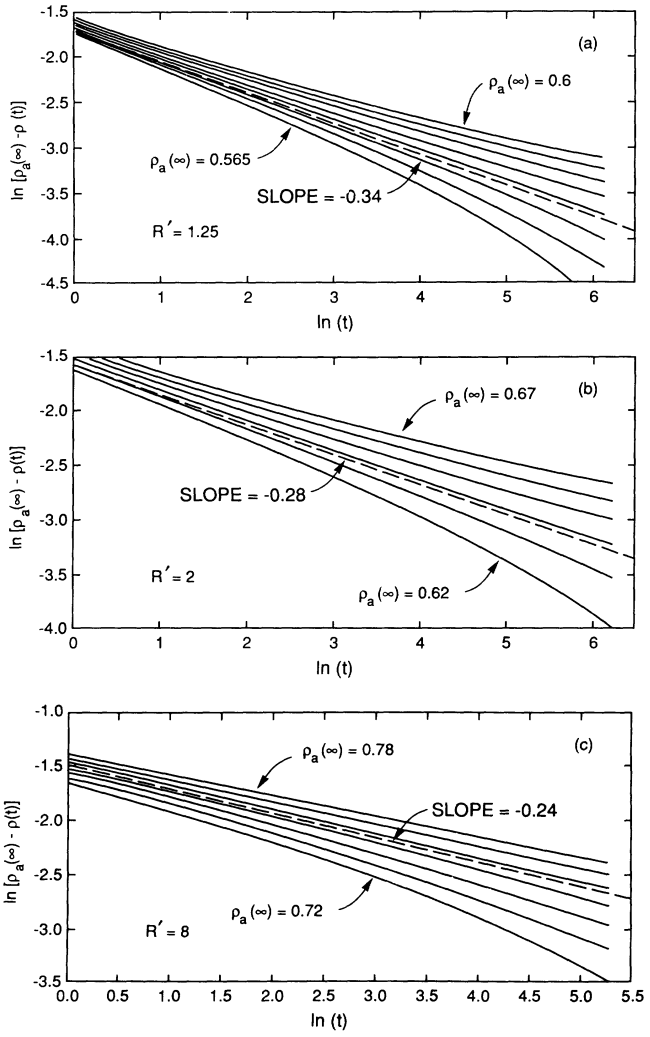

FIG. 7. Dependence of $\ln[\rho_a(\infty)-\rho(t)]$ on $\ln(t)$ for the simulations illustrated in Fig. 6. Each curve corresponds to a different value of $\rho_a(\infty)$. (a), (b), and (c) show results for a size distribution parameter (R') of 1.25, 2.0, and 8.0, respectively.

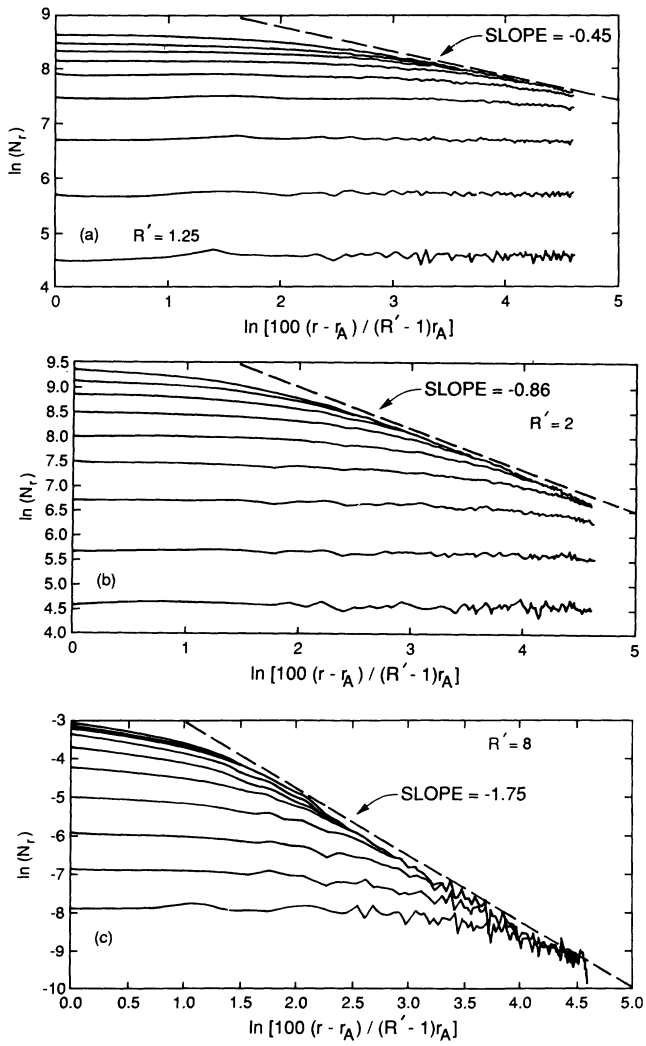

FIG. 8. Adsorbed disk radius distributions at several stages during the simulations shown in Figs. 6 and 7. The data is the same as that displayed in Fig. 6 but here the dependence of $\ln(N_r)$ on $\ln\{[100(r-r_A)]/[R'-1)r_A]\}$ is shown.

R'. In additions to the results shown in Fig. 8, values for γ of 0.67, 1.22, 1.36, and 1.64 were obtained for $R'=1.5$, 3.0, 4.0, and 6.0, respectively.

In these simulations a disk with a radius r given by

$$r=r_A+x(r_B-r_A) \tag{14}$$

was first selected and then an attempt was made to add it to the planar substrate. In Eq. (14) x is a random number uniformly distributed over the range $0<x<1$. Simulations with nonuniform distributions in which the disk radii were given by

$$r=r_A+x^{\eta}(r_B-r_A) \tag{15}$$

were also carried out for several values of the exponent η.

Results from the truncated-Gaussian-distribution model

In the Gaussian-distribution model disk radii are selected randomly from a Gaussian distribution given by

$$P(r)=e^{[-(r-\bar{r})^2/a^2]}. \tag{16}$$

An attempt is made to add the randomly selected disk to the planar substrate and the disk is "adsorbed" if it does not overlap with other disks. Disks with radii smaller than $\bar{r}-5a$ were assigned radii of $\bar{r}-5a$ and disks with radii larger than $\bar{r}+5a$ were assigned radii of $\bar{r}+5a$. It is uncommon to find disks with radii smaller than $\bar{r}-5a$ or larger than $\bar{r}+5a$ and this truncation of the Gaussian distribution has a negligible effect on our simulation results.

Figures 9(a), 9(b), and 9(c) show the distributions of adsorbed disk radii (N_r) obtained with three different values for the width parameter (a) in Eq. (16) [$a=0.025\bar{r}$, $0.01\bar{r}$, and $0.175\bar{r}$ in Figs. 9(a), 9(b), and 9(c), respectively]. Figure 9(d) shows the distribution of adsorbed disk radii taken from 11 simulations using a broad Gaussian distribution ($a=0.175\bar{r}$). The simulations were carried out on systems of size 1024×1024. The disk radii varied from 0.7075 ($\bar{r}-5a$) to 10.6125 ($\bar{r}+5a$). Figure 9(d) shows the size distribution at the latest stage.

At the early stages in the RSA process the distribution of adsorbed disks is Gaussian, which reflects the Gaussian distribution of the disks that are fed to the surface. For small values of the polydispersity parameter (a) the distribution remains more or less Gaussian and the mean radius decreases slightly as the RSA process proceeds. For large values of a this shift is large and the distribution of adsorbed disk radii becomes very non-Gaussian [Figs. 9(c) and 9(d)].

Figure 10 shows the dependence of $\ln[\rho_a(\infty)-\rho(t)]$ on $\ln(t)$ for several values of $\rho_a(\infty)$ for the broadest distribution studied here ($a=0.175\bar{r}$). Figure 10 indicates that if the approach of $\rho(t)$ to its asymptotic value can be described by Eq. (9), then the exponent ρ has a very large value. This is consistent with the theoretical results of Tarjus and Talbot [47] since $\rho(r)$ and its derivatives at $r=r_{\min}=\bar{r}-5a$ have essentially zero values and the effective value of n in Eq. (11) is large.

Narrow size distributions

Since two-dimensional random-sequential adsorption has been studied experimentally using particles (polymer microspheres) that are almost monodisperse it is impor-

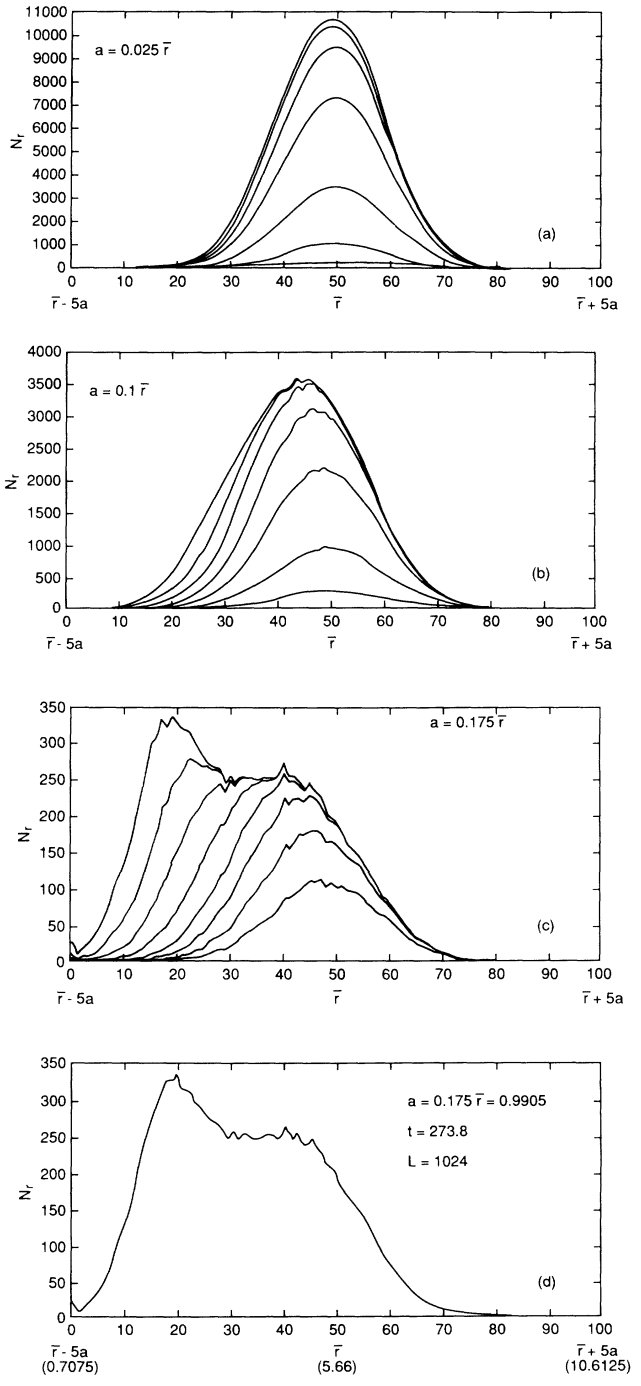

FIG. 9. Distribution of adsorbed disk radii obtained from simulations carried out using the Gaussian-distribution model. (a), (b), and (c) show the disk radii distributions at several stages during simulations carried out with width parameters (a) of $0.025\bar{r}$, $0.1\bar{r}$, and $0.175\bar{r}$, respectively. (d) shows the distribution of adsorbed disk radii taken from 11 simulations with $a=0.175\bar{r}$ at a late stage.

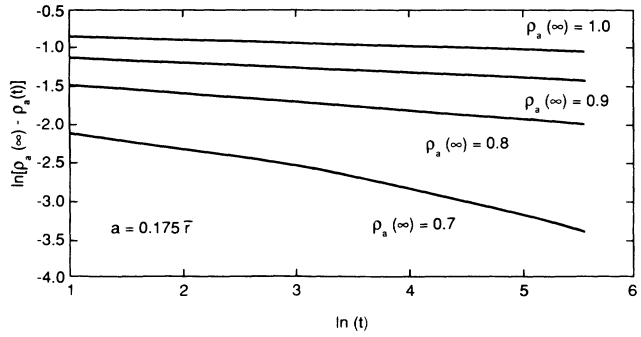

FIG. 10. Dependence of $\ln[\rho_a(\infty)-\rho(t)]$ on $\ln(t)$ obtained from simulations carried out using the Gaussian-distribution model with a large polydispersity ($a=0.175\bar{r}$).

tant to investigate how the monodisperse limit is approached in polydisperse RSA. Unfortunately, this limit is difficult to approach in computer simulations. Results from the binary mixture model as the limit $R\rightarrow 1$ is approached have been described above.

A series of simulations was carried out using the uniform radius distribution model with small values for $R'-1$ ($R'-1\leq 0.4$). For small values of $(R'-1)$ our simulation results and the theoretical arguments of Tarjus and Talbot indicate that the RSA kinetics can be represented quite well by Eq. (11), [i.e., $p=\frac{1}{3}$ and $q=0$ in Eq. (2)]. Consequently, the asymptotic ($t\rightarrow\infty$) coverage was obtained using Eq. (11). Figure 11 shows the dependence of $\ln[\rho(R',\infty)]$ on $\ln(R'-1)$ obtained from these simulations. Here $\rho(R',\infty)$ is the asymptotic coverage for radius distribution parameter of R'. Figure 11 indicates that the asymptotic coverage increases with polydispersity according to the power law

$$\rho(R',\infty)-\rho(1,\infty)\sim(R'-1)^{\lambda}, \tag{17}$$

where the exponent λ has a value of about 0.84 in the limit $R'\rightarrow 1$. The effective value of this exponent is quite close to 1.0 and an asymptotic ($R'\rightarrow 1$) exponent of 1.0

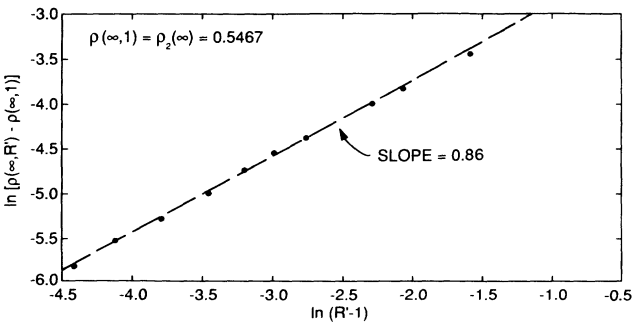

FIG. 11. Dependence of the asymptotic ($t\rightarrow\infty$) coverage $[\rho(R',\infty)]$ on the polydispersity parameter (R') obtained from simulations carried out using the uniform radius distribution model. Here the dependence of $\ln[\rho(R',\infty)-\rho(1,\infty)]$ on $\ln(R'-1)$ is show [where $\rho(1,\infty)$ is the monodisperse coverage $\rho_2(\infty)$].

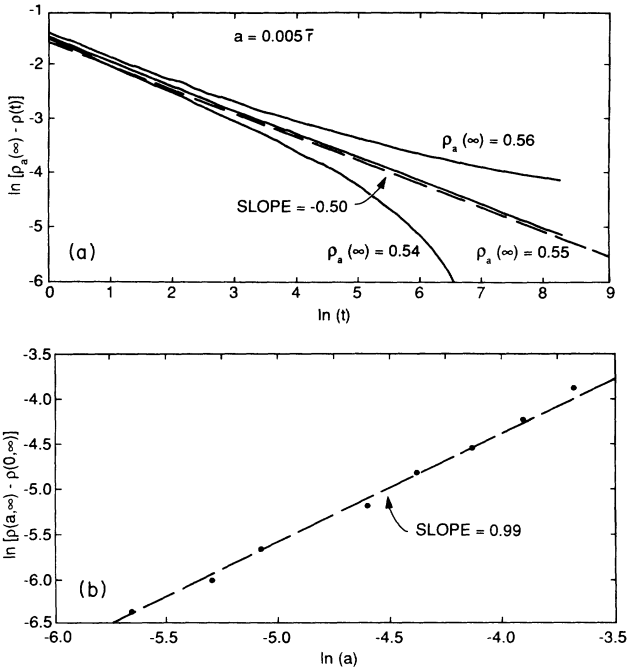

FIG. 12. Results from the Gaussian-distribution model with small polydispersities. (a) shows the dependence of $\ln[\rho_a(\infty)-\rho(t)]$ on $\ln(t)$ for $a=0.005\bar{r}$, where $\rho_a(\infty)$ represents "test" values for the asymptotic ($t\rightarrow\infty$) coverage. (b) shows the dependence of $\ln[\rho(\infty,a)-\rho(\infty,0)]$ on $\ln(a)$.

cannot be excluded by these simulations.

Similar simulations were carried out using the Gaussian-distribution model with small polydispersities. For this model the effective value of the exponent p in Eq. (2) appears to depend on the polydispersity parameter (a), but for very small values of a an effective value of about $\frac{1}{2}$ is obtained [Fig. 12(a)]. Consequently, the asymptotic coverage was estimated assuming that $\rho=\frac{1}{2}$. This introduces substantial uncertainties but the dependence of $\ln[\rho(a,\infty)-\rho(0,\infty)]$ on $\ln(a)$ obtained in this manner is shown in Fig. 12(b). From this figure it appears that

$$\rho(a,\infty)-\rho(0,\infty)\sim a^{\lambda'}, \tag{18}$$

where the exponent λ' has an effective value of about 1.0. Here $\rho(0,\infty)$ is the asymptotic coverage at zero polydispersity $[\rho_2(\infty)]$. Each data point in Fig. 12(b) was obtained from several simulations in which attempts were made to add 4×10^8 disks to an area of 512×512.

SUMMARY

The random-sequential adsorption of objects with a distribution of shapes and/or sizes has become a subject of considerable interest in recent years. Much of the theoretical effort has been devoted to the $R\rightarrow\infty$ limit for binary mixtures. This is an important limit that may be experimentally accessible. However, most of the experi-

mental studies of random-sequential adsorption have been carried out using either macromolecules or polymer microspheres with only a narrow distribution of sizes. Consequently, the approach to the $R \rightarrow 1$ limit may be of more immediate practical importance. The general binary RSA problem and the polydisperse RSA process appear to pose major theoretical challenges and we may have to be content with computer-simulation results such as those described here for quite some time.

For the monodisperse RSA process, the jamming limit coverage can be obtained by first carrying out standard RSA simulations until the jamming limit is approached. At this stage, holes that are large enough to contain disks are then identified and filled [27]. However, these holes may overlap and it is difficult to fill them in an efficient fashion without introducing bias into the procedure or resorting to a complex algorithm. In any event there is no evidence that the value for $\rho_2(\infty)$ obtained in this manner is any more reliable than that obtained by extrapolating $\rho_2(t)$ to $t = \infty$ using Feder's law. For the polydisperse RSA problem both procedures are more difficult and the challenge of obtaining results from polydisperse RSA that are as reliable as those obtained for the monodisperse RSA problem still remains. Fortunately, the rapid pace of computer technology should enable us to obtain results that are adequate for comparison with foreseeable experiments and useful for testing most theoretical results using a "brute force" approach. However, the development of more efficient RSA algorithms would be a worthwhile undertaking.

[1] P. J. Flory, J. Am. Chem. Soc. **61**, 1518 (1939).
[2] E. R. Cohen and H. Reiss, J. Chem. Phys. **38**, 680 (1963).
[3] J. J. Gonzalez, P. C. Hemmer, and J. S. Hoye, Chem. Phys. **3**, 228 (1974).
[4] I. R. Epstein, Biopolymers **18**, 765 (1979).
[5] J. K. Mackenzie, J. Chem. Phys. **37**, 723 (1962).
[6] J. W. Evans, D. R. Burgess, and D. K. Hoffman, J. Chem. Phys. **79**, 5011 (1983).
[7] J. W. Evans and R. S. Nord, Phys. Rev. B **31**, 1759 (1985).
[8] G. C. Barker and M. J. Grimson, Mol. Phys. **63**, 145 (1988).
[9] Y. Fan and Y. K Percus, Phys. Rev. Lett. **67**, 1677 (1991).
[10] M. Tanemura, Am. Inst. Stat. Math. **31**, 351 (1979).
[11] L. Finegold and J. T. Donnell, Nature (London) **278**, 443 (1979).
[12] J. Feder, J. Theor. Biol. **87**, 237 (1980).
[13] J. Feder and I. Giaver, J. Colloid Interface Sci. **78**, 144 (1980).
[14] G. Y. Onoda and E. G. Liniger, Phys. Rev. A **33**, 715 (1986).
[15] J. Ugelstad, A. Berge, R. Schmidt, P. Stenstad, and A. T. Skjeltorp in *Polymer Reaction Engineering*, edited by K. H. Reichert and W. Geiseler (Huthig and Wepf, Heidelberg, 1986).
[16] H. Solomon, Proc. Berkeley Symp. Math. Stat. Probab. **3**, 119 (1967).
[17] D. W. Cooper, Phys. Rev. A **38**, 522 (1988).
[18] D. W. Cooper, J. Colloid Interface Sci. **119**, 442 (1987).
[19] K. Gotoh, W. S. Jodrey, and E. M. Tory, Powder Technol. **21**, 285 (1978).
[20] B. Widom, J. Chem. Phys. **44**, 3888 (1966).
[21] A. Reyni, Sel. Trans. Math. Stat. Prob. **4**, 203 (1963).
[22] P. Meakin, J. L. Cardy, E. Loh, and D. J. Scalapino, J. Chem. Phys. **86**, 2380 (1987).
[23] J. W. Evans and R. S. Nord, Phys. Rev. A **31**, 3831 (1985).
[24] J. W. Evans and R. S. Nord, Phys. Rev. B **31**, 1759 (1985).
[25] R. H. Swendsen, Phys. Rev. A **24**, 504 (1981).
[26] Y. Pomeau, J. Phys. A **13**, L193 (1980).
[27] E. L. Hinrichsen, J. Feder, and T. Jossang, J. Stat. Phys. **44**, 793 (1986).
[28] J. Talbot, G. Tarjus, and P. Schaff, Phys. Rev. A **40**, 4808 (1980).
[29] R. D. Vigil and R. M. Ziff, J. Chem. Phys. **91**, 2599 (1989).
[30] B. J. Brosilow, R. M. Ziff, and R. D. Vigil, Phys. Rev. A **43**, 631 (1991).
[31] P. Schaaf and J. Talbot, Phys. Rev. Lett. **62**, 175 (1989).
[32] G. C. Barnum and M. J. Grimson, Mol. Phys. **63**, 175 (1989).
[33] J. W. Evans, Phys. Rev. Lett. **62**, 2642 (1989).
[34] M. Henkel and N. M. Svrakic (unpublished).
[35] N. M. Svrakic and M. Henkel (unpublished).
[36] R. Dickman, J.-S. Wang, and I. Jensen (unpublished).
[37] A. Barman and D. Kvitasov, J. Phys. A **22**, L251 (1989).
[38] V. Privman, J.-S. Wang, and P. Nielaba, Phys. Rev. B **43**, 3366 (1991).
[39] S. S. Manna and N. M. Svrakic (unpublished).
[40] J. D. Sherwood, J. Phys. A **23**, 2827 (1990).
[41] M. C. Bartelt and V. Privman, J. Chem. Phys. **93**, 6820 (1990).
[42] R. D. Vigil and R. M. Ziff, J. Chem. Phys. **93**, 8270 (1990).
[43] R. M. Ziff and R. D. Vigil, J. Phys. A **23**, 5103 (1990).
[44] P. Nielaba, V. Privman, and J.-S. Wang, J. Phys. A **23**, L1187 (1990).
[45] P. Nielaba, V. Privman, and J.-S. Wang, Phys. Rev. B **43**, 3366 (1990).
[46] J. Talbot and P. Schaaf, Phys. Rev. A **40**, 422 (1989).
[47] G. Tarjus and J. Talbot, J. Phys. A **24**, L913 (1991).
[48] E. L. Hinrichsen, Ph.D. thesis, University of Oslo, 1989.
[49] M. C. Bartelt and V. Privman, Phys. Rev. A **44**, R2227 (1991).